RESEARCH ARTICLE

Continuous theta-burst stimulation of the right superior temporal gyrus impairs self-motion perception

A. A. Tarnutzer · A. G. Lasker · D. S. Zee

Abstract Sensory input from the semicircular canals (SCC) and otolith organs is centrally combined with signals from other sensory modalities to continuously update the internal estimate of self-motion. Constant velocity vertical on-axis rotation leads to decay of the nystagmus response from the horizontal SCC and of perceived angular velocity (PAV), and when the rotation stops, a similar oppositely directed post-rotatory response occurs. Case reports and electrical stimulation studies suggest an involvement of the temporo-peri-Sylvian vestibular cortex in generating the PAV. Here, we transiently inhibited the right superior temporal gyrus (STG) by use of continuous theta-burst stimulation (cTBS) and predicted an accelerated decay of PAV compared to controls ($n = 5$ control session first, $n = 1$ cTBS session first). Constant velocity (100°/s) vertical on-axis rotations were applied over 75 s before (1 block) and after (3 blocks) cTBS over the right STG in six subjects. Breaks between the rotations (75 s) were initiated by abrupt stops. By use of a rotating potentiometer, subjects indicated the PAV during and after the chair rotations. Simultaneously eye positions were recorded using a scleral search coil. One subject was excluded for per-rotary analysis. Early after cTBS, the post-rotary PAV decay time constant (DTC) was significantly (9.4 ± 5.7 vs. 13.6 ± 5.9 s; $p = 0.049$) reduced (no directionality to this effect observed). Overall, post-rotary PAV showed a trend toward shortened DTC compared to the control trials ($p = 0.086$) in the first 25 min after cTBS, while per-rotary PAV was not significantly changed. Per-rotary and post-rotary aVOR

DTC were not significantly changed after cTBS ($p > 0.05$). These findings support the hypothesis that the right STG is involved in mediating self-motion perception and can be modulated by cTBS.

Keywords Vestibular · Angular vestibulo-ocular reflex · Transcranial magnetic stimulation · Eye movements

Introduction

Self-motion in space is continuously monitored by the central nervous system and strongly depends on vestibular input from both the semicircular canals (SCC, for detection of rotations) and the otolith organs (for detection of translations and tilt). These sensory estimates are processed within the brainstem vestibular nuclei and the cerebellum. Being forwarded to the cerebral cortex, vestibular input is then combined with other sensory signals (vision, proprioception), contributing to a unified and continuously updated internal estimate of self-motion (Straube and Brandt 1987; Kahane et al. 2003; Angelaki et al. 2009). On-axis rotation along an earth-vertical axis (=yaw) evokes a vestibulo-perceptual response and a vestibulo-ocular response, the angular vestibulo-ocular reflex (aVOR), resulting in compensatory SCC-driven horizontal eye movements, which aim at stabilizing the eyes in space. During prolonged constant velocity rotations, both responses decay approximately exponentially. When the subject is then abruptly stopped, the aVOR and the percept of self-rotation immediately re-emerge, however, now pointing in the opposite direction. Subsequently, the post-rotary vestibulo-ocular (Benson 1968; Buttner and Waespe 1981; Cohen et al. 1981) and vestibulo-perceptual (Okada et al. 1999; Sinha et al. 2008) responses again decay exponentially with a decay time

A. A. Tarnutzer (✉) · A. G. Lasker · D. S. Zee
Department of Neurology, The Johns Hopkins University
School of Medicine, Path 2-210, 600 N. Wolfe St., Baltimore,
MD 21201, USA
e-mail: atarnutzer@gmail.com

constant (DTC) of approximately 15–20 s. However, at the same time, it has been shown in non-human primates that the DTC of the head velocity signal in the vestibular nerve is only 7–10 s (Buttner and Waespe 1981). Thus, the head velocity signal is stored centrally (Buettner et al. 1978) and released to ocular motor neurons and to cerebral cortical areas involved in vestibular perception (Okada et al. 1999). A so-called velocity storage mechanism carries out this integration of the head velocity signal (Raphan et al. 1979) and is regulated by midline cerebellar structures capable of modifying the vestibulo-ocular DTC (Cohen et al. 1992, 2002). For the percept of self-motion, additional neural processing beyond the velocity storage mechanism of the aVOR—probably located within the cerebral cortex—has been proposed (Sinha et al. 2008).

Clinical findings in epileptic patients (Penfield and Jasper 1954; Smith 1960; Wieser 1991; Fish et al. 1993; Munari et al. 1995; Galimberti et al. 1998; Kluge et al. 2000; Erbayat Altay et al. 2005) and observations derived from cortical lesions (Brandt et al. 1994, 1995; Israel et al. 1995), from caloric and galvanic stimulation (Friberg et al. 1985; Bottini et al. 1994; Bucher et al. 1998; Lobel et al. 1998; Bense et al. 2001; Suzuki et al. 2001; Deutschlander et al. 2002; Fasold et al. 2002; Eickhoff et al. 2006; Lopez et al. 2012) and from evoked potentials (de Waele et al. 2001), suggest a widely distributed bilateral multisensory cortical vestibular system. Based on functional imaging (Dieterich and Brandt 2008) and electrical stimulation studies (Penfield and Jasper 1954; Wieser 1991; Kahane et al. 2003), this network seems to be centered bilaterally around the Sylvian fissure in the posterior insula, the superior temporal gyrus (STG), the inferior parietal lobule, the pre- and post-central gyrus, the adjacent inferior frontal gyrus and the anterior cingulate gyrus (Eickhoff et al. 2006). Kahane et al. (2003) coined the term "temporo-peri-Sylvian vestibular cortex (TPSVC)" to describe this area based on its functional and anatomical properties. Electrical stimulation within the TPSVC evoked illusions of rotation, translation or indefinable feelings of body motion (Penfield and Jasper 1954; Kahane et al. 2003) and vertigo accompanied by nausea was described in a patient with a ganglioma in the right STG (Paduch et al. 1999). According to PET studies during caloric irrigation and functional MRI (fMRI) studies with galvanic and optokinetic stimulation in healthy human subjects and in patients with vestibular lesions, there is evidence that the vestibular cortical network is activated more strongly in the non-dominant hemisphere (Dieterich and Brandt 2008).

Based on these studies, a significant contribution of the TPSVC including the STG to self-motion perception is predicted, with the vestibular cortical network being more active on the right side than on the left side. However, electrical stimulation is invasive and limited in its availability and lesion-based case series often report on diverse patient populations with heterogeneous and non-focal lesion locations. Furthermore, these patients typically can only be examined in the subacute or chronic state. Noteworthy, adaptation in response to such lesions gradually evolves and makes a distinction between the effects of lesions and of central compensation in these patients difficult.

To overcome these limitations and to study the functional implications of circumscribed areas of the brain, transcranial magnetic stimulation (TMS) has increasingly been used, as transient inhibition or excitation of targeted areas of the brain can be achieved non-invasively [for an extensive review of TMS see (Rossi et al. 2009)], creating a "virtual lesion" in the first case. We hypothesized that transiently inhibiting those cortical areas related to generating the internal estimate of angular velocity by use of repetitive TMS (rTMS) applying a continuous theta-burst stimulation (cTBS) protocol may lead to altered vestibulo-perceptual, but not vestibulo-ocular responses, as the roles of the cerebral cortex in vestibular perception and control of the vestibulo-ocular reflex are not identical (Brandt et al. 1994). In this study, we aimed to temporally inhibit the right STG to determine the effect of vestibular cortical cTBS on per- and post-rotary (i) self-motion perception and (ii) aVOR, at a time point when adaptation is evolving or even before it starts. We expected attenuated self-motion perception (as reflected in a reduced DTC) when temporarily inhibiting vestibular cortical areas involved in head velocity perception. Vestibulo-ocular responses, at the same time, should be unchanged or modulated independently since they are likely mediated by mechanisms distinct from those involved in generating the percept of self-motion (Brandt et al. 1994; Merfeld et al. 2005; Palla et al. 2008; Seemungal et al. 2011; Haburcakova et al. 2012).

Materials and methods

Subjects

Six right-handed healthy human subjects aged between 26 and 65 years (mean $\pm$ 1 SD: 43 $\pm$ 19 years) were studied. Handedness was determined by a 13-item questionnaire (Chapman and Chapman 1987), and all subjects studied were right-handed according to this questionnaire. Informed written consent of all participants was obtained after full explanation of the experimental procedure. The protocol was approved by the Johns Hopkins Institutional Review Board and was in accordance with the Declaration of Helsinki for research involving human subjects.
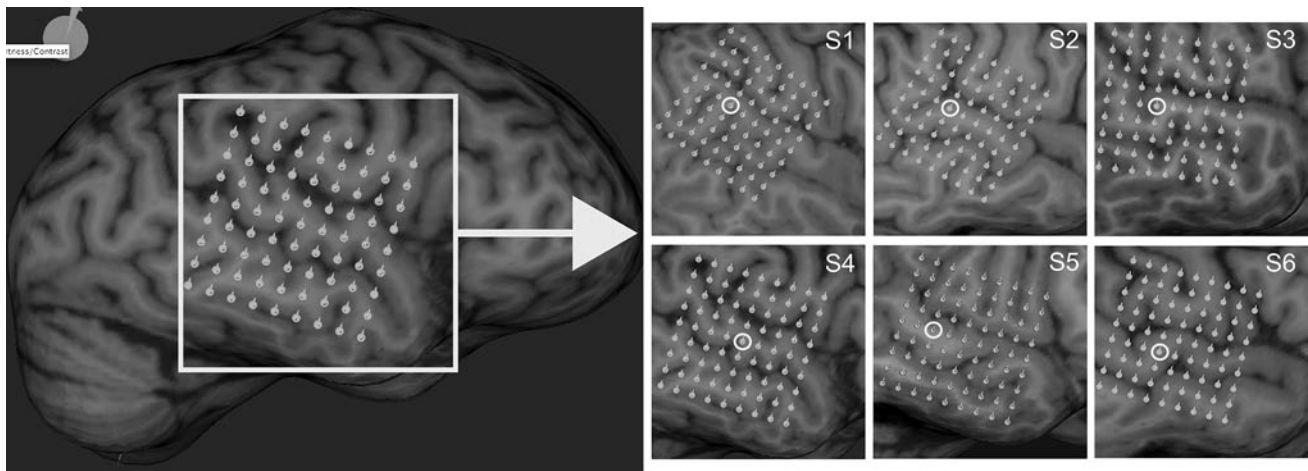
Fig. 1 Illustration of the individually selected cTBS stimulation site (*white circles*) based on the surface reconstruction of the MRI scan provided by the neuronavigation software (Brainsight 2.0.7; The Rogue Company, Canada). While the panel on the left provides an overview of the selected right temporo-parietal area, the smaller panels on the right indicate the individual stimulation sites, being positioned over the right STG in all subjects

Experimental setup

All participants obtained a structural MRI scan (sagittal MPRAGE-sequence, 3T). All MRI scans were evaluated by a board-certified neuroradiologist to identify any pathologies which may exclude subjects from participation in the study. Target selection and TMS coil positioning were based on neuronavigation (Brainsight 2.0.7; The Rogue Company, Canada). We used a Magstim Superrapid TMS device (The Magstim Company Ltd, Whitland, UK) and a first generation Magstim double coil (70 mm diameter; The Magstim Company Ltd) for all experiments.

The active motor threshold (AMT) of the left first digital interosseous muscle (FDI) using biphasic single-pulse TMS over the contralateral motor cortex was determined in each subject according to internationally accepted criteria (≥ 5 out of 10 responses with a peak-to-peak compound muscle activity potential [CMAP] of 200 μV or more during slight voluntary contraction of the contralateral FDI). We used a Bagnoli 2-channel EMG-system (DelSys Inc., Boston, USA) and interactive programs written in MATLAB 7 (The MathWorks, Natick, USA) to record and display the CMAPs elicited by single-pulse TMS.

For continuous theta-burst stimulation (cTBS), we used the protocol by Huang and colleagues [200 bursts at a frequency of 5 Hz with 3 pulses per burst at a frequency of 50 Hz, 600 pulses in total (Huang et al. 2005)], which lasts approximately 40 s at a power of 80 % of the individual's AMT. For motor evoked potentials, this protocol has been shown to result in a pronounced and prolonged suppression that reaches a maximum about 5–10 min after the end of the protocol and that may last 30 or even 60 min. The TMS

coil handle was positioned in such a way that it was pointing upwards and that the flow of current was perpendicular to the orientation of the right STG. The coil was positioned in this way based on previous observations that single-pulse TMS over the primary motor cortex yielded larger CMAPs when the current flow was perpendicular to the orientation of the precentral gyrus (Brasil-Neto et al. 1992; Mills et al. 1992). Based on preliminary data from our laboratory, case reports (Paduch et al. 1999; Hegemann et al. 2004) and electric cortical stimulation studies (Kahane et al. 2003; Best et al. 2010), we selected the right posterior STG (approximately 1–2 cm posterior to the central sulcus) as stimulation site (see Fig. 1) in all subjects. The location of the coil during the 40-s cTBS run was monitored by neuronavigation; drifts of the TMS coil off target were less than 3 mm in all subjects.

All experiments were collected in darkness with the subject sitting upright in a rotating chair with the head fixed in an upright and straight ahead position by use of an individually molded bite bar. The head was horizontal by definition when a horizontal laser line was parallel to both lower lids. Subjects indicated the sensed direction and speed of chair and body rotation (termed "perceived angular velocity" or PAV) by turning a handle that was connected to a potentiometer recording the handle position. This potentiometer was built according to the potentiometer used in the Zurich vestibulo-oculomotor laboratory, Switzerland, for all self-motion perception studies. Its reliability had been demonstrated in various studies (Bertolini et al. 2011, 2012). The potentiometer was attached to the subjects' right thigh using Velcro strap, and subjects were asked to hold the box with their left hand while moving the handle

with their dominant right hand. Subjects used the hand ipsilateral to the side of cTBS for indicating the direction and speed of self-motion. Therefore, potential modulations of right-hemispheric areas related to motor control (e.g., primary motor cortex) should not influence the motor performance of the behavioral task. Three dimensional eye movements were recorded using a single scleral search coil (Chronos Vision, Berlin, Germany). The search coil was calibrated beforehand. Further details of the calibration and eye movement recording procedures may be found in (Bergamin et al. 2001; Ramat and Zee 2003).

A questionnaire was provided right before and about 30 min after cTBS to assess potential side effects as dizziness, vertigo, nausea or headache. In general, mostly mild side effects may be observed in about 5 % of subjects after cTBS (Oberman et al. 2011). Furthermore, due to the right temporal location of cTBS, we also evaluated for visuo-spatial neglect by use of a line bisection task, a line cancelation task and a figure copying task (Ogden 1985).

Experimental setting

All six subjects completed a control session (no TMS) and a test session with cTBS over the right posterior STG. Note that one subject (S3) later was excluded for the analysis of the per-rotary data sets, however, and was included for the analysis of the post-rotary paradigms. The two sessions were at least 48 h apart. Five subjects completed first the control session (S1, S2, S3, S5 and S6), while one (S4) received the test session before the control session. In each session, we obtained a series of chair rotations (termed "block") four times. Subjects were always rotated along an earth-vertical axis with an acceleration of $100°/s^2$ and a constant velocity of $100°/s$. Each block consisted of four phases, each lasting 75 s, resulting in a total duration per block of 5 min. The four phases are described in detail in Fig. 2.

During all four phases (i.e., both per- and post-rotary), ocular motor (horizontal aVOR) and perceptual responses (PAV) were recorded at a frequency of 1000 Hz. Subjects were asked to indicate their *sensed* direction and speed of body rotation by turning the handle attached to the potentiometer during all four phases of each block. In either session, we obtained four blocks with 3-min breaks in between blocks. During the breaks, the lights were turned on and additional artificial tears and local anesthetics were administered on the left eye if required. Whereas in the test session TBS-stimulation (T0) was applied between block 1 (baseline) and block 2, no TMS was applied in the control session. Before the first block, a practice block was run to familiarize subjects with the equipment. During the blocks, subjects were further instructed to look straight ahead and to blink regularly.

Data analysis

Recorded raw eye, chair and potentiometer position signals were processed and analyzed using MATLAB 7 (The MathWorks, Natick, MA). Zero-phase forward and reverse digital filtering (filtfilt.m, MATLAB 7) was performed on the calibrated eye position traces using a Gaussian filter with a width of 51 samples (from center to 2 % of height, singlesided). Eye and disk velocity obtained by differentiating and filtering eye and disk position traces were further processed. A running mean and standard deviation (SD; sample width: 20) was calculated for all trials. Data points deviating more than 1 SD from the running mean were considered outliers and were removed. The decision to set the cutoff to 1 SD was based on preliminary data analysis showing that selecting a larger cutoff (e.g., 2 SD) in our data set impaired the fitting algorithm considerably. All resulting eye and disk velocity traces were then processed interactively to remove additional data points considered as outliers based on visual
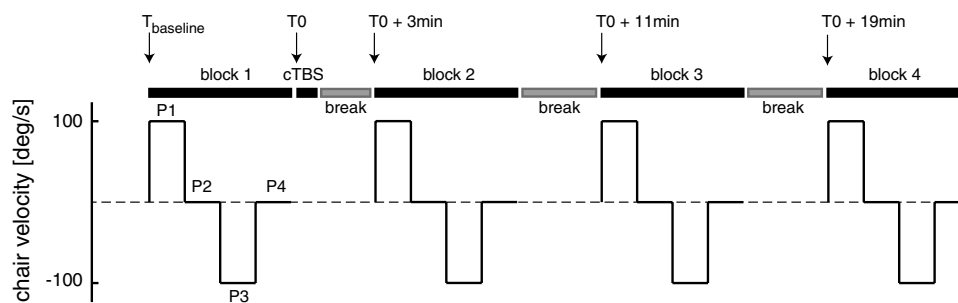
Fig. 2 Graphical illustration of stimulation paradigm on the rotating chair. Chair velocity is plotted against time, with positive values referring to clockwise (CW) rotations and negative values indicating counter-clockwise (CCW) chair rotations. Each block consisted of a sequence of four phases (P1–P4), each lasting 75 s: P1: constant velocity CW chair rotation; P2: post-rotary period; P3: constant velocity CCW chair rotation; P4: post-rotary period. For the TMS session, cTBS was applied after the first block at time T0. After cTBS, 3 blocks were applied at T0 + 3 min, T0 + 11 min and T0 + 19 min. Breaks of 3 min separated these three blocks. The *dashed line* refers to zero chair velocity
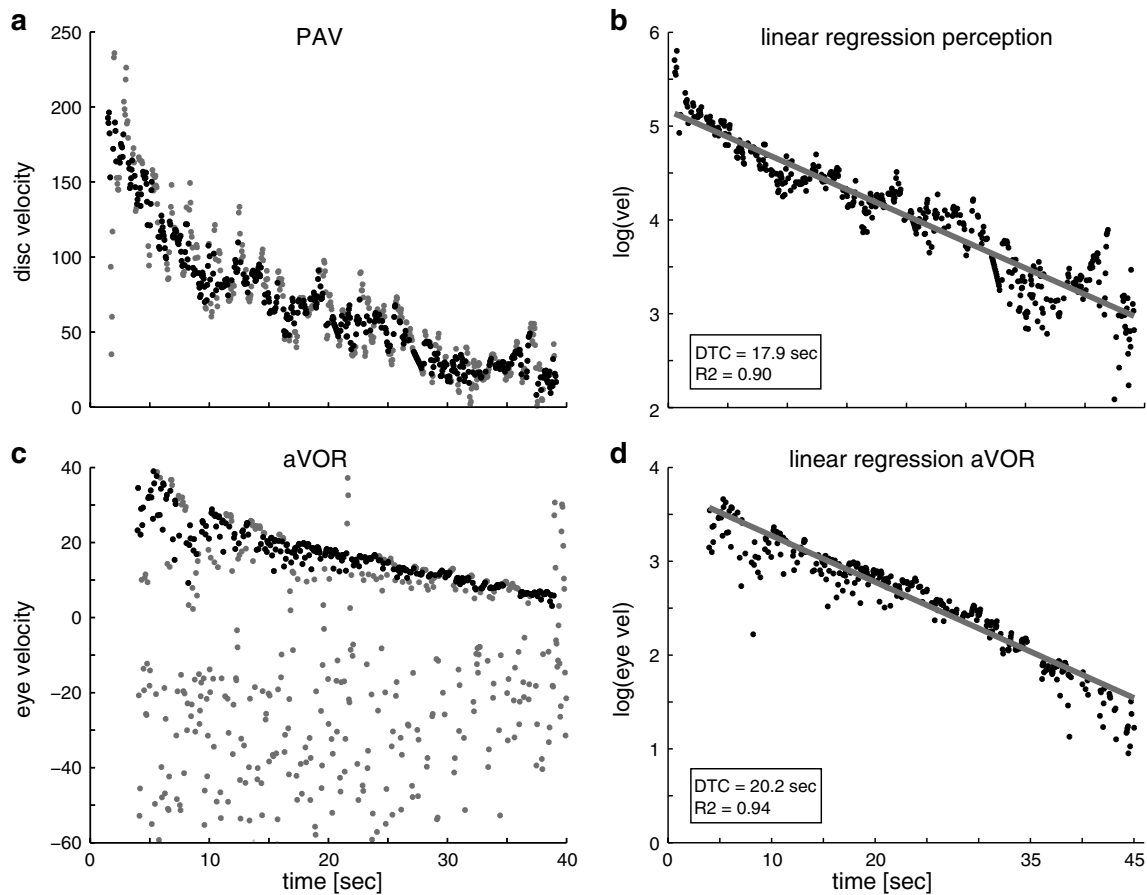
Fig. 3 Single raw traces (s6) for both perceived angular velocity (PAV) and the angular vestibulo-ocular reflex (aVOR) illustrating the removal of outliers (**a**, **c**, *gray dots*) and the linear regression analysis on the traces (**b**, **d**). Note that traces focus on the decay period, i.e., data points during the initial rise period are not considered. Disk

(**a**) and eye (**b**) velocity plotted against time, indicating outliers (*gray dots*) and selected data points (*black dots*). Linear regression analysis on the selected data points for the disk (**c**) and the eye (**d**), with the fit in gray and the fitting results (R^2 value and decay time constant DTC) in insets

inspection. Note that interactive removal of outliers was restricted to few data points and blocks. Figure 3 shows exemplary raw PAV and aVOR velocity traces before and after automatized removal of outliers.

Both aVOR and perceived angular velocity (PAV) responses were analyzed in terms of their dynamics, including the time from onset of nystagmus or disk rotation to maximal velocity (rise time) and the decay time by calculating the exponential decay time constant (DTC). To determine the DTC, we applied a linear least square regression analysis using robustfit.m (MATLAB 7, The MathWorks, Natick, USA) on the logarithm of eye and disk velocity data (Okada et al. 1999). We also provide R^2 values reflecting the goodness of fit along with the DTC. Fitting was restricted from the time of maximal velocity to the time point when the disk or eye velocity decreased below 2 SD (i.e., below 4.5 %) from the maximal velocity (=100 %)—defined as the median over the five data points with highest velocities for at least 500 ms.

Since repetitive constant velocity chair rotations may result in short-term habituation of the aVOR (Cohen et al. 1992) and likely also of the perceptual response, we compared results from runs 2–4 relative to the baseline run 1. Furthermore, we compensated for possible, inherent fluctuations in DTC by offsetting the DTCs obtained from run 1 in both the control and test conditions in such a way that they were of equal size. The same offsets were then added to the DTC of runs 2–4 in both conditions. Only after these adjustments, DTC of runs 2–4 of the TMS and control condition were compared. Statistical analysis was obtained using paired *t* tests, and Bonferroni correction was applied to take multiple comparisons into account.

Results

All six subjects completed both sessions. Stimulation intensity for cTBS was 44 or 45 %, which reflected 80 % of the

individually determined AMT. However, in two subjects, the designated stimulation intensity for cTBS was above the 45 % power level limit of the TMS device available. Therefore, in S3 (cTBS at 78 % of AMT) and S6 (cTBS at 74 % of ATM), the stimulation intensity was slightly below the targeted 80 % of ATM.

None of the subjects indicated any illusionary (translational or rotational) movements after cTBS. Small to moderate ipsilateral facial nerve stimulation was noted in most subjects; however, none of them reported these sensations to be painful. Noteworthy, no other side effects related either to the TMS procedure or to the scleral search coil, including nausea, tension-type headache or blurred vision, were noticed by any of the subjects. Screening for visuospatial neglect approximately 30 min after cTBS based on the Ogden-figure, a line cancelation task and a line bisection task were negative in all subjects.

In a first step, we evaluated the quality of the linear fits to the eye and perception velocity traces using robustfit.m (see methods section for details). As direction of chair rotation did not have a significant effect (paired t tests, $p > 0.05$) on the R^2 values for both per- and post-rotary aVOR and PAV traces, CW and CCW chair rotations were pooled for further analysis of goodness of fit. Overall quality of fit was high for both PAV and aVOR traces, yielding R^2 values of 0.85 ± 0.10 and 0.89 ± 0.08 (mean $\pm$ 1 SD; per-rotary and post-rotary traces) for PAV and R^2 values of 0.86 ± 0.13 and 0.86 ± 0.14 for per-rotary and post-rotary aVOR. Time-to-peak disk and eye velocity were determined in all runs and yielded similar average values (± 1 SD) for both PAV (2.1 ± 1.8 s) and aVOR (1.6 ± 1.3 s). Noteworthy, PAV time-to-peak was comparable to those values previously observed by our group (Sinha et al. 2008). Search coil calibration sequences were obtained at the beginning of the session, about 5 min after cTBS and at the end of each session (about 30 min after cTBS). To evaluate for possible TMS-induced eye movements, these calibration files were searched for nystagmus. Noteworthy, we did not find any nystagmus in the calibration sequences obtained after cTBS application.

Decay time constant analysis

Decay time constants (DTC) of PAV and aVOR were calculated for all individual subjects, and per-rotary and post-rotary phases were analyzed separately.

Post-rotary conditions

Exemplary single subject velocity traces (subject S2) illustrating both the perceptual and the ocular motor response before and after cTBS are shown in Fig. 4. While the DTC of the perceptual response is diminished after cTBS,
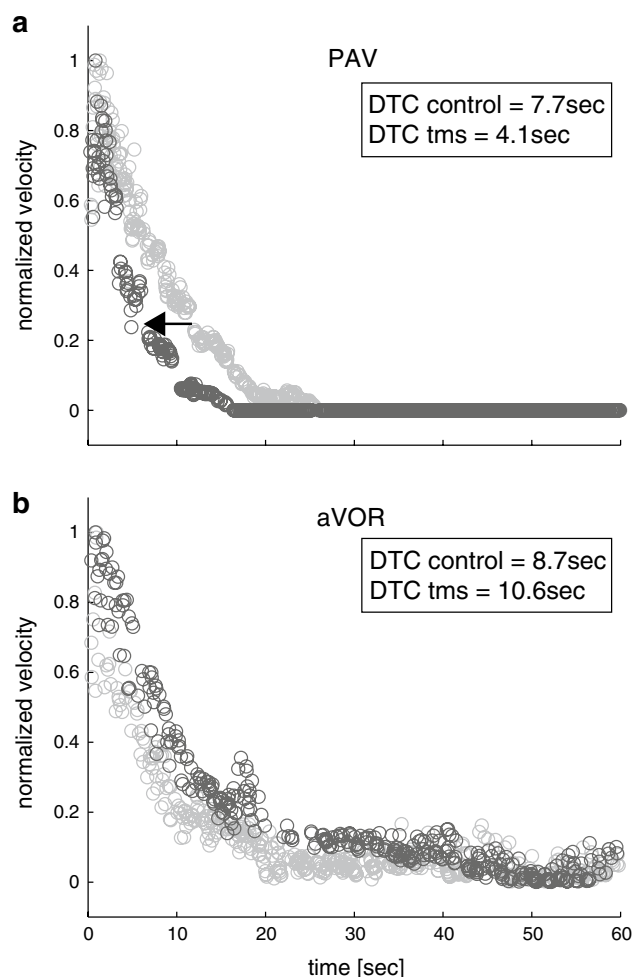

Fig. 4 Single raw traces (S2) from both the control (in *light gray*) and the test (in *dark gray*) condition showing the impact of cTBS on the PAV (**a**) and the aVOR (**b**). **a** After cTBS, the DTC was reduced by 53 %, as reflected in a steeper decay of the slope. The *black arrow* illustrates the shift in the PAV curve. **b** After cTBS, no reduction in DTC could be found, rather it increased by 22 % in this trial

the aVOR DTC shows a tendency to be increased in this subject.

Individual aVOR and PAV DTC values relative to the baseline DTC are shown for both preceding CW and CCW chair rotations separately in Fig. 5. Both for trials with CW and CCW chair rotations, PAV DTCs were reduced after cTBS (runs 2–4) in 4 out of 6 subjects compared to the baseline (run 1). In the remaining two subjects each, this was not or only partially the case (S1 and S3 for CW; S3 and S6 for CCW) as illustrated in Fig. 5.

For post-rotary trials (pooling runs 1–4), the direction of preceding chair rotation did not affect the DTC of the aVOR and the PAV (paired t test, $p > 0.05$). This was true for both the control and the TMS session. We therefore pooled trials with preceding CW and CCW chair rotation
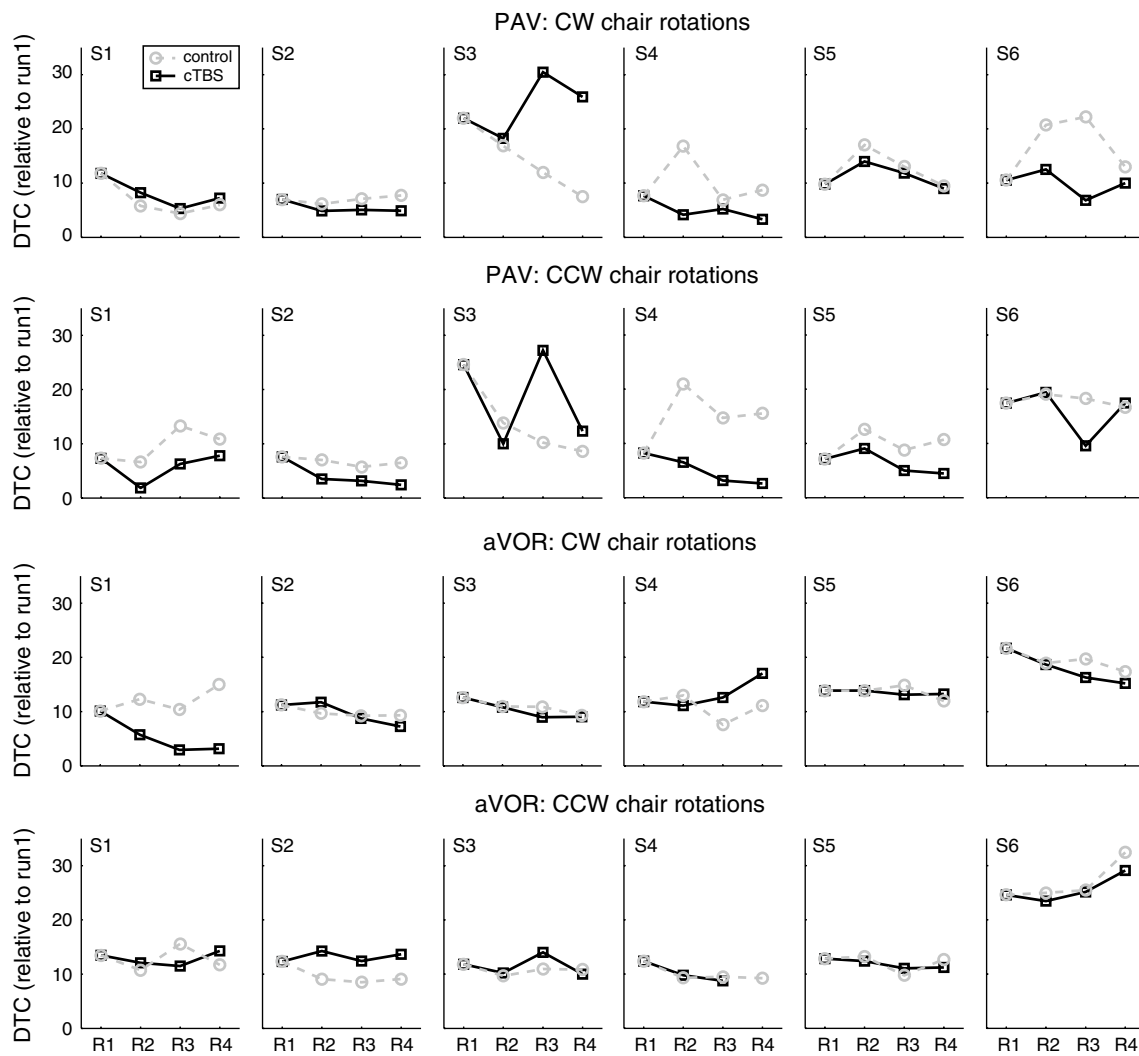
Fig. 5 Individual decay time constants of both post-rotary PAV and aVOR are shown for all six subjects (S1-S6) and CW and CCW chair rotations separately, comparing DTC before (*gray circles*, interconnected with *dashed line*) and after cTBS (*black squares*, interconnected with *solid line*) in runs R1–R4. Note that offsets of the baseline runs of the control and cTBS session were nulled to allow comparison

for further analysis of the PAV and the aVOR. As stated in the methods, DTCs of the control and TMS condition were aligned in such a way that the baseline DTC values were identical to allow a direct comparison of the two sessions. As we were interested in quantifying the effect of TMS on DTC, we focused on the runs after TMS (runs 2–4) and their companions in the control session (see Fig. 6b). Statistical analysis showed overall (pooling data from runs 2–4) a trend toward shorter PAV DTCs values after cTBS (paired t test, $p = 0.086$). A subgroup analysis, comparing the three different runs separately, again using paired t tests and compensating for multiple tests by use of Bonferroni correction, indicated a significant reduction in PAV DTCs after cTBS only in run 2 ($p = 0.049$), while this was not the case for runs 3 ($p = 0.63$) and 4 ($p = 0.60$) as illustrated

in Fig. 7. Noteworthy, the lack of significant differences in runs 3 and 4 and when pooling runs 2, 3 and 4 was mainly a result from the response characteristics of subject S3 (see individual PAV data of S3 in Fig. 4 for details). At the same time, aVOR DTC after cTBS (see Fig. 6d) did not significantly change relative to the control session when pooling runs 2, 3 and 4 or when analyzing runs 2, 3 and 4 separately.

Per-rotary conditions

For the analysis of the data sets obtained while the chair was rotating, we had to remove one subject (S3), as this subject continued to rotate the disk as long as the chair was moving, despite the fact that we instructed all subjects
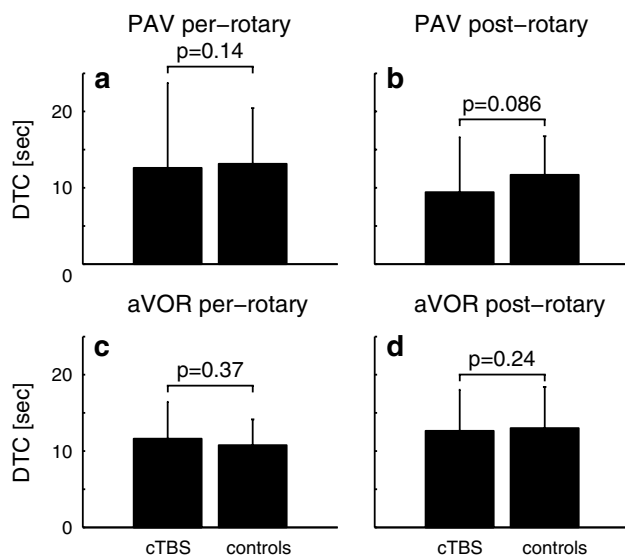
Fig. 6 Overall DTC (pooling CW and CCW trials and runs 2–4) for both the PAV and the aVOR during (per-rotary, $n = 5$ subjects) and immediately after (post-rotary, $n = 6$ subjects) constant velocity chair rotation along the yaw-axis, comparing decay times for the control and the cTBS condition. Note that only for the PAV post-rotary (**b**) there was a trend for reduced DTC after cTBS, while in all other conditions, p values were larger than 0.1
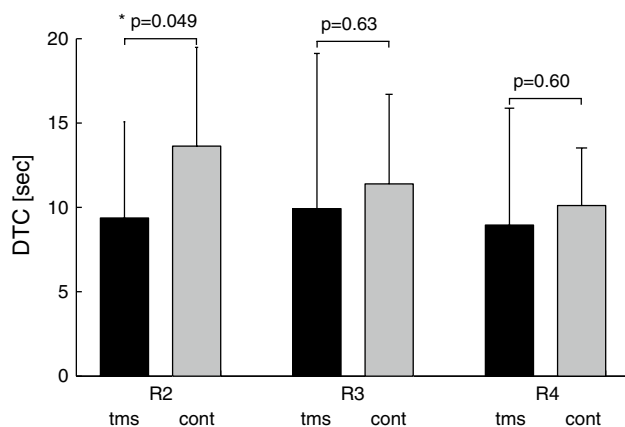
Fig. 7 PAV post-rotary decay time constants of runs 2–4 are shown both for the control (*gray bars*) and the cTBS (*black bars*) condition. A significant (*) decrease of DTC was noted only for run 2. Note that trials with CW and CCW chair rotation were pooled as DTC did not depend on the direction of preceding chair yaw rotation

to focus on the sensed body motion rather than on external cues as the noise or the air circulation induced by the rotating chair. Compared to the post-rotary traces, the inter-individual differences in PAV and aVOR DTC were markedly larger, making this data set more difficult to analyze.

In the five subjects included for the analysis of the per-rotary phases, the direction of chair rotation did not have a significant effect (paired t test, $p > 0.05$) on the DTC

(including data from runs 1–4) of the aVOR and PAV. For further analysis of the DTC, therefore, runs with CW and CCW chair rotation were pooled. Again, we focused on the effect of cTBS on the DTC; therefore, comparison between the two sessions was restricted to runs 2, 3 and 4. Noteworthy, statistical analysis did not show any significant differences of PAV or aVOR in the per-rotary conditions, as illustrated in panels a and c of Fig. 6.

Discussion

In this study, we aimed at modulating the internal estimate of self-motion, as presumably generated within the temporo-peri-Sylvian vestibular cortex (TPSVC), including the right superior temporal gyrus (STG) by use of inhibitory repetitive transcranial magnetic stimulation (continuous theta-burst stimulation protocol, cTBS). We predicted temporally attenuated self-motion perception after cTBS, as reflected by a decrease in the decay time constant (DTC) of perceived angular velocity (PAV). Indeed, early after cTBS post-rotary PAV was found to decay significantly faster compared to the control condition, suggesting a relevant contribution of the right STG to the integration of vestibular signals and the generation of self-motion perception. At the same time, the angular vestibulo-ocular reflex (aVOR) remained unaffected by cTBS.

The role of the STG in perceiving angular velocity

The cortical areas involved in generating the internal estimate of self-motion and spatial orientation have been extensively studied [see (DeAngelis and Angelaki 2012) for review]. Brain surface electrical stimulation studies (Kahane et al. 2003) and single case reports with focal lesions (Paduch et al. 1999; Hegemann et al. 2004) leading to vestibular sensations and functional imaging studies [see (Dieterich and Brandt 2008) and (Lopez et al. 2012) for reviews] indicated the involvement of both temporal and parietal lobe areas along the Sylvian fissure, including the posterior insula and the STG. Within this large area, different vestibular sensations (e.g., rotations along different axes) may be elicited at different locations (Kahane et al. 2003). To our best knowledge, the concept of non-invasively inducing a "virtual lesion" within the temporal "vestibular" cortical areas by use of rTMS has not been applied before.

In principal, self-motion perception can be measured in terms of perceived rotational velocity or angular displacement. Sensed angular displacement is the integral of estimated angular velocity (Goldberg and Fernandez 1971a, b; Buttner and Waespe 1981). Velocity and acceleration signals arising from the vestibular and the somatosensory

system are integrated over time to provide an estimate of displacement. This process is called path integration (Loomis et al. 1999). Parietal cortex rTMS suggested contralateral encoding of perceived angular displacement with a right-hemispheric bias (Philbeck et al. 2006; Seemungal et al. 2008). Specifically, rTMS over the posterior parietal cortex disrupted path integration but not velocity perception, indicating that there might be separate areas that process vestibular signals of head velocity versus those involved in path integration (Seemungal et al. 2008). Taking our findings into account, the right posterior STG is likely part of the vestibular cortical network contributing to velocity perception. In our data set, we observed a significant reduction in PAV DTC only in the first 5–10 min after cTBS, whereas based on the previous literature (although focusing on the primary motor cortex), a longer lasting effect, reaching 30–60 min (Huang et al. 2005; Gentner et al. 2008; Oberman et al. 2011), could be expected. While this observation might suggest a shorter effect of cTBS on vestibular cortical areas, it may also be explained by the increasing inter-individual variability in runs 3 and 4 and the relatively small sample size.

PET studies during caloric irrigation and functional MRI (fMRI) studies with galvanic and optokinetic stimulation in healthy human subjects and in patients with vestibular lesions demonstrated that the vestibular cortical network is activated more strongly in the non-dominant hemisphere (Dieterich and Brandt 2008). Noteworthy, we applied cTBS only to the non-dominant (right) hemisphere and selected the posterior STG as target area. Taking into account that we did not observe any direction-dependent changes of PAV, this finding suggests that the right STG may be contributing to self-motion perception for both CW and CCW rotations. This lack of lateralization effects for right-sided inhibition within the TPSVC is consistent with findings in previous studies: Small case series of patients with right-hemispheric lesions affecting parts of the "vestibular" cortical areas showed impaired perception of both CW and CCW rotations, while in case of left-hemispheric lesions, only CW rotations were perceived inaccurately (Philbeck et al. 2006). This observation underlines the dominant role of the right hemisphere, suggesting that it is involved in the processing of rotational stimuli into either direction. However, the lack of directional differences in PAV after cTBS may theoretically also be a result of the relatively small number of subjects and trials obtained in our study and the inter-individual variability of DTCs measured.

Previously, interruption of biological motion perception (i.e., the recognition of human action depicted in sparse dot displays) has been reported after patterned TMS (either standard rTMS or cTBS) over the posterior superior temporal sulcus, which delineates the STG and the middle temporal gyrus (Grossman et al. 2005; van Kemenade et al.

2012). This proposes a relevant contribution of the STG and its adjacent sulcus to motion processing across modalities, integrating both visual and vestibular motion stimuli, and is in agreement with our findings.

The discrepancy between significantly shortened PAV DTC early after cTBS in the post-rotary trials and the lack of significant changes at the same time period in the per-rotary trials is likely a result of the larger inter-individual variability of PAV in the per-rotary trials. Additional sensory cues in the per-rotary trials as provided by chair vibration, noise and air flow may have contributed to this increase in variability. This might have obscured effects of cTBS when assessing the PAV while the chair is rotating.

The aVOR decay time constant remained unchanged after cTBS

Unlike the PAV, the aVOR was unchanged after cTBS over the right STG. While the percept of self-motion is a higher cognitive function, being generated within the "vestibular" cortex, the aVOR is governed by a brainstem–cerebellar network centered on the vestibular nuclei. However, the cortical vestibular network does not only receive ascending pathways from the vestibular nuclei but also projects back to these brainstem nuclei as observed in non-human primates (Guldin and Grusser 1998). Such reciprocal connections potentially allow a cortical modulation of the brainstem aVOR as summarized in (Arshad et al. 2013). Indeed, such a cortical influence on vestibular function was demonstrated in healthy human subjects for cognitive tasks such as bistable perception and attention tasks [resulting in asymmetrical aVOR DTCs (Arshad et al. 2013)] or when focusing on imaginary targets moving together with the own body while rotating [resulting in aVOR gain decreases (Barr et al. 1976)]. In patients with unilateral visuo-spatial neglect and lesions involving the occipito-temporo-parietal junction, asymmetrical aVOR gains (Doricchi et al. 2002; Ventre-Dominey et al. 2003), altered aVOR time constants (Ventre-Dominey et al. 2003) and optokinetic responses (Doricchi et al. 2002) were reported. Importantly, the patients included in these studies had chronic, heterogeneous and more extensive cortical lesions than induced by cTBS [affecting few cm^2 of brain tissue located under the coil or less (Roth et al. 1991; Thielscher and Kammer 2004)]. Noteworthy, direction-specific changes in aVOR DTC (with faster decay for rotations toward the lesioned hemisphere) seem to depend on the presence of visuo-spatial neglect, as DTC remained symmetrical in both patients without hemineglect (Ventre-Dominey et al. 2003) and in the healthy participants of this study, which were all screened negative for neglect after cTBS. Furthermore, we did not apply any cognitive tasks known to be effective in altering the aVOR DTC.

Limitations

Limitations in this pilot study included a small number of participants and considerable inter-individual variability in the perceptual responses. As a result, the statistical power to detect significant differences in DTC was limited. This may provide an explanation for the moderate impact only of cTBS on the PAV. Noteworthy, repetitive indications of PAV may induce habituation as observed for the aVOR (Cohen et al. 1992), resulting in decreased DTC in subsequent trials solely due to training effects. This potential confound was addressed by aligning both sessions based on their baseline DTC values. By keeping the two sessions at least 48 h apart, potential habituation induced by brief stimulation periods would likely have diminished, so that the baseline adjustments are expected to be independent from each other.

The effect of TMS on the brain tissue underneath the TMS coil is only partially understood. The majority of TMS research has been focused on the primary motor cortex, as the resulting response—the compound muscle action potential—can be quantified reliably. This includes the cTBS protocol applied here (Huang et al. 2005), which has been originally designed to modulate the primary motor cortex. Depending on the cytological architecture of the targeted brain tissue (including the orientation of the nerve fibers relative to the surface and the density of neurons), other, non-motor cortical areas may be more or less prone to standard cTBS protocols. Also, objective and quantifiable output parameters are missing for rTMS over non-motor areas. The moderate changes in PAV after cTBS over the right STG may therefore potentially be related to these cortical areas being less prone to TMS, underestimating the role of the STG in self-motion processing when applying cTBS.

Furthermore, the brain volume affected by TMS is limited (with a surface diameter of a few centimeters or less for a standard figure-of-eight coil) and not exactly known. This is especially true for the depth of penetration of TMS. Simulations showed a fast decay of field strength with stimulation depth (Thielscher and Kammer 2004). Therefore, cortical areas further away from the surface are more difficult to stimulate sufficiently with TMS. Considering the size of the cortical areas associated with the processing of vestibular sensory input, focal inhibition by use of TMS may not be disruptive enough to provoke a more complete impairment of self-motion processing, explaining the moderate changes in PAV DTC observed here.

Conclusions

In this pilot study, we showed that cTBS over the right STG may elicit a transient virtual lesion, resulting in a moderate—but significant—shortening of the percept of self-motion in the first 5–10 min after cTBS, while the aVOR remained unaffected. These results provide further support for the role of the right STG in the processing of rotational stimuli and match previous patient data, including intraoperative surface electrical stimulation responses. cTBS of the STG may therefore provide a useful model to simulate lesions within the cortical vestibular areas and the compensatory changes by the brain. Taking into account the pilot study character of this work, inclusion of a larger study sample is encouraged for future studies addressing the role of the STG in vestibular perception.

References

Angelaki DE, Gu Y, DeAngelis GC (2009) Multisensory integration: psychophysics, neurophysiology, and computation. Curr Opin Neurobiol 19:452–458

Arshad Q, Nigmatullina Y, Bronstein AM (2013) Handedness-related cortical modulation of the vestibular-ocular reflex. J Neurosci 33:3221–3227

Barr CC, Schultheis LW, Robinson DA (1976) Voluntary, non-visual control of the human vestibulo-ocular reflex. Acta Otolaryngol 81:365–375

Bense S, Stephan T, Yousry TA, Brandt T, Dieterich M (2001) Multisensory cortical signal increases and decreases during vestibular galvanic stimulation (fMRI). J Neurophysiol 85:886–899

Benson AJ (1968) Postrotational sensation and nystagmus as indicants of semicircular canal function. In: Third symposium on the role of the vestibular organs in space exploration, Washington (DC): Office of technology utilization national aeronautics and space administration

Bergamin O, Zee DS, Roberts DC, Landau K, Lasker AG, Straumann D (2001) Three-dimensional Hess screen test with binocular dual search coils in a three-field magnetic system. Invest Ophthalmol Vis Sci 42:660–667

Bertolini G, Ramat S, Laurens J, Bockisch CJ, Marti S, Straumann D, Palla A (2011) Velocity storage contribution to vestibular self-motion perception in healthy human subjects. J Neurophysiol 105:209–223

Bertolini G, Ramat S, Bockisch CJ, Marti S, Straumann D, Palla A (2012) Is vestibular self-motion perception controlled by the velocity storage? Insights from patients with chronic degeneration of the vestibulo-cerebellum. PLoS ONE 7:e36763

Best C, Stefan H, Hopfengaertner R, Dieterich M (2010) Effects of electrical stimulation in vestibular cortex areas in humans. J Neurol Sci 290:157–162

Bottini G, Sterzi R, Paulesu E et al (1994) Identification of the central vestibular projections in man: a positron emission tomography activation study. Exp Brain Res 99:164–169

Brandt T, Dieterich M, Danek A (1994) Vestibular cortex lesions affect the perception of verticality. Ann Neurol 35:403–412

Brandt T, Botzel K, Yousry T, Dieterich M, Schulze S (1995) Rotational vertigo in embolic stroke of the vestibular and auditory cortices. Neurology 45:42–44

Brasil-Neto JP, McShane LM, Fuhr P, Hallett M, Cohen LG (1992) Topographic mapping of the human motor cortex with magnetic stimulation: factors affecting accuracy and reproducibility. Electroencephalogr Clin Neurophysiol 85:9–16

Bucher SF, Dieterich M, Wiesmann M, Weiss A, Zink R, Yousry TA, Brandt T (1998) Cerebral functional magnetic resonance imaging of vestibular, auditory, and nociceptive areas during galvanic stimulation. Ann Neurol 44:120–125

Buettner UW, Buttner U, Henn V (1978) Transfer characteristics of neurons in vestibular nuclei of the alert monkey. J Neurophysiol 41:1614–1628

Buttner U, Waespe W (1981) Vestibular nerve activity in the alert monkey during vestibular and optokinetic nystagmus. Exp Brain Res 41:310–315

Chapman LJ, Chapman JP (1987) The measurement of handedness. Brain Cogn 6:175–183

Cohen B, Henn V, Raphan T, Dennett D (1981) Velocity storage, nystagmus, and visual-vestibular interactions in humans. Ann N Y Acad Sci 374:421–433

Cohen H, Cohen B, Raphan T, Waespe W (1992) Habituation and adaptation of the vestibuloocular reflex: a model of differential control by the vestibulocerebellum. Exp Brain Res 90:526–538

Cohen B, John P, Yakushin SB, Buettner-Ennever J, Raphan T (2002) The nodulus and uvula: source of cerebellar control of spatial orientation of the angular vestibulo-ocular reflex. Ann N Y Acad Sci 978:28–45

de Waele C, Baudonniere PM, Lepecq JC, Tran Ba Huy P, Vidal PP (2001) Vestibular projections in the human cortex. Exp Brain Res 141:541–551

DeAngelis GC, Angelaki DE (2012) Visual–vestibular integration for self-motion perception. In: Murray MM, Wallace MT (eds) The neural bases of multisensory processes, chap 31. CRC Press, Boca Raton

Deutschlander A, Bense S, Stephan T, Schwaiger M, Brandt T, Dieterich M (2002) Sensory system interactions during simultaneous vestibular and visual stimulation in PET. Hum Brain Mapp 16:92–103

Dieterich M, Brandt T (2008) Functional brain imaging of peripheral and central vestibular disorders. Brain 131(Pt 10):2538–2552. doi:10.1093/brain/awn042

Doricchi F, Siegler I, Iaria G, Berthoz A (2002) Vestibulo-ocular and optokinetic impairments in left unilateral neglect. Neuropsychologia 40:2084–2099

Eickhoff SB, Weiss PH, Amunts K, Fink GR, Zilles K (2006) Identifying human parieto-insular vestibular cortex using fMRI and cytoarchitectonic mapping. Hum Brain Mapp 27:611–621

Erbayat Altay E, Serdaroglu A, Gucuyener K, Bilir E, Karabacak NI, Thio LL (2005) Rotational vestibular epilepsy from the temporo-parieto-occipital junction. Neurology 65:1675–1676

Fasold O, von Brevern M, Kuhberg M, Ploner CJ, Villringer A, Lempert T, Wenzel R (2002) Human vestibular cortex as identified with caloric stimulation in functional magnetic resonance imaging. Neuroimage 17:1384–1393

Fish DR, Gloor P, Quesney FL, Olivier A (1993) Clinical responses to electrical brain stimulation of the temporal and frontal lobes in patients with epilepsy. Pathophysiological implications. Brain 116(Pt 2):397–414

Friberg L, Olsen TS, Roland PE, Paulson OB, Lassen NA (1985) Focal increase of blood flow in the cerebral cortex of man during vestibular stimulation. Brain 108(Pt 3):609–623

Galimberti CA, Versino M, Sartori I, Manni R, Martelli A, Tartara A (1998) Epileptic skew deviation. Neurology 50:1469–1472

Gentner R, Wankerl K, Reinsberger C, Zeller D, Classen J (2008) Depression of human corticospinal excitability induced by magnetic theta-burst stimulation: evidence of rapid polarity-reversing met plasticity. Cereb Cortex 18:2046–2053

Goldberg JM, Fernandez C (1971a) Physiology of peripheral neurons innervating semicircular canals of the squirrel monkey. 3. Variations among units in their discharge properties. J Neurophysiol 34:676–684

Goldberg JM, Fernandez C (1971b) Physiology of peripheral neurons innervating semicircular canals of the squirrel monkey. I. Resting discharge and response to constant angular accelerations. J Neurophysiol 34:635–660

Grossman ED, Battelli L, Pascual-Leone A (2005) Repetitive TMS over posterior STS disrupts perception of biological motion. Vision Res 45:2847–2853

Guldin WO, Grusser OJ (1998) Is there a vestibular cortex? Trends Neurosci 21:254–259

Haburcakova C, Lewis RF, Merfeld DM (2012) Frequency dependence of vestibuloocular reflex thresholds. J Neurophysiol 107:973–983. doi:10.1152/jn.00451.2011

Hegemann S, Fitzek S, Fitzek C, Fetter M (2004) Cortical vestibular representation in the superior temporal gyrus. J Vestib Res 14:33–35

Huang YZ, Edwards MJ, Rounis E, Bhatia KP, Rothwell JC (2005) Theta burst stimulation of the human motor cortex. Neuron 45:201–206

Israel I, Rivaud S, Gaymard B, Berthoz A, Pierrot-Deseilligny C (1995) Cortical control of vestibular-guided saccades in man. Brain 118(Pt 5):1169–1183

Kahane P, Hoffmann D, Minotti L, Berthoz A (2003) Reappraisal of the human vestibular cortex by cortical electrical stimulation study. Ann Neurol 54:615–624

Kluge M, Beyenburg S, Fernandez G, Elger CE (2000) Epileptic vertigo: evidence for vestibular representation in human frontal cortex. Neurology 55:1906–1908

Lobel E, Kleine JF, Bihan DL, Leroy-Willig A, Berthoz A (1998) Functional MRI of galvanic vestibular stimulation. J Neurophysiol 80:2699–2709

Loomis JM, Klatzky RL, Golledge RG, Philbeck JW (1999) Human navigation by path integration. In: Golledge RG (ed) Wayfinding behavior: cognitive mapping and other spatial processes. Johns Hopkins Press, Baltimore, pp 125–151

Lopez C, Blanke O, Mast FW (2012) The human vestibular cortex revealed by coordinate-based activation likelihood estimation meta-analysis. Neuroscience 212:159–179

Merfeld DM, Park S, Gianna-Poulin C, Black FO, Wood S (2005) Vestibular perception and action employ qualitatively different mechanisms. II. VOR and perceptual responses during combined Tilt&Translation. J Neurophysiol 94:199–205

Mills KR, Boniface SJ, Schubert M (1992) Magnetic brain stimulation with a double coil: the importance of coil orientation. Electroencephalogr Clin Neurophysiol 85:17–21

Munari C, Berta E, Minotti L et al (1995) Contribution to the identification of "vestibular" cortex in man: a stereo EEG study. In: Collard M, Jeannerod M, Christen Y (eds) Le cortex vestibulaire. Irvinn, Strasbourg, pp 48–63

Oberman L, Edwards D, Eldaief M, Pascual-Leone A (2011) Safety of theta burst transcranial magnetic stimulation: a systematic review of the literature. J Clin Neurophysiol 28:67–74

Ogden JA (1985) Contralesional neglect of constructed visual images in right and left brain-damaged patients. Neuropsychologia 23:273–277

Okada T, Grunfeld E, Shallo-Hoffmann J, Bronstein AM (1999) Vestibular perception of angular velocity in normal subjects and in patients with congenital nystagmus. Brain 122(Pt 7):1293–1303

Paduch T, Baborie A, Krauss JK (1999) Bifocal temporal gangli-oglioma. Neurosurg Rev 22:112–116

Palla A, Straumann D, Bronstein AM (2008) Vestibular neuritis: ver-tigo and the high-acceleration vestibulo-ocular reflex. J Neurol 255:1479–1482. doi:10.1007/s00415-008-0935-2

Penfield W, Jasper H (1954) Epilepsy and the functional anatomy of the human brain. Little, Brown, Boston

Philbeck JW, Behrmann M, Biega T, Levy L (2006) Asymmetrical perception of body rotation after unilateral injury to human ves-tibular cortex. Neuropsychologia 44:1878–1890

Ramat S, Zee DS (2003) Ocular motor responses to abrupt interaural head translation in normal humans. J Neurophysiol 90:887–902

Raphan T, Matsuo V, Cohen B (1979) Velocity storage in the vestib-ulo-ocular reflex arc (VOR). Exp Brain Res 35:229–248

Rossi S, Hallett M, Rossini PM, Pascual-Leone A (2009) Safety, ethi-cal considerations, and application guidelines for the use of tran-scranial magnetic stimulation in clinical practice and research. Clin Neurophysiol 120:2008–2039

Roth BJ, Saypol JM, Hallett M, Cohen LG (1991) A theoretical calcu-lation of the electric field induced in the cortex during magnetic stimulation. Electroencephalogr Clin Neurophysiol 81:47–56

Seemungal BM, Rizzo V, Gresty MA, Rothwell JC, Bronstein AM (2008) Posterior parietal rTMS disrupts human Path Integration during a vestibular navigation task. Neurosci Lett 437:88–92

Seemungal BM, Masaoutis P, Green DA, Plant GT, Bronstein AM (2011) Symptomatic recovery in miller fisher syndrome parallels vestibular-perceptual and not vestibular-ocular reflex function. Front Neurol 2:2. doi:10.3389/fneur.2011.00002

Sinha N, Zaher N, Shaikh AG, Lasker AG, Zee DS, Tarnutzer AA (2008) Perception of self motion during and after passive rota-tion of the body around an earth-vertical axis. Prog Brain Res 171:277–281

Smith BH (1960) Vestibular disturbances in epilepsy. Neurology 10:465–469

Straube A, Brandt T (1987) Importance of the visual and vestibular cortex for self-motion perception in man (circularvection). Hum Neurobiol 6:211–218

Suzuki M, Kitano H, Ito R et al (2001) Cortical and subcortical ves-tibular response to caloric stimulation detected by functional magnetic resonance imaging. Brain Res 12:441–449

Thielscher A, Kammer T (2004) Electric field properties of two com-mercial figure-8 coils in TMS: calculation of focality and effi-ciency. Clin Neurophysiol 115:1697–1708

van Kemenade BM, Muggleton N, Walsh V, Saygin AP (2012) Effects of TMS over premotor and superior temporal cortices on biologi-cal motion perception. J Cogn Neurosci 24:896–904

Ventre-Dominey J, Nighoghossian N, Denise P (2003) Evidence for interacting cortical control of vestibular function and spatial rep-resentation in man. Neuropsychologia 41:1884–1898

Wieser HG (1991) Ictal manifestations of temporal lobe seizures. Adv Neurol 55:301–315